



Bootstrapping spectra: Methods, comparisons and application to knock data

Abdelhak M. Zoubir

Signal Processing Group, Technische Universität Darmstadt, Merckstr. 25, D-64283 Darmstadt, Germany

ARTICLE INFO

Article history:

Received 25 June 2009

Received in revised form

29 November 2009

Accepted 30 November 2009

Dedicated to J.F. Böhme on the occasion
of his 70th birthday

Available online 11 December 2009

Keywords:

Bootstrap

Confidence interval

Spectral density

Periodogram

Autoregressive process

Knock

ABSTRACT

The problem of confidence interval estimation for spectra is addressed. Unlike asymptotic techniques, bootstrap techniques provide accurate measures of confidence in that they maintain the preset level, in particular for small sample sizes and non-Gaussian data. We investigate some recently proposed methods, a time domain bootstrap approach, the so-called tapered block bootstrap and a combined time domain and frequency domain approach, the so-called autoregressive-aided periodogram bootstrap. We compare the methods with a well-established frequency domain residual based bootstrap technique in view of confidence accuracy. Confidence interval estimates for spectra of knock data are shown.

© 2009 Elsevier B.V. All rights reserved.

1. Introduction

Consider a real-valued, discrete-time, strictly stationary univariate process X_t , $t \in \mathbb{Z}$, that admits the representation (see [3,15])

$$X_t = \sigma \sum_{\tau=-\infty}^{\infty} h_{\tau} \varepsilon_{t-\tau}, \quad t \in \mathbb{Z}, \quad (1)$$

where $\{h_{\tau}\}$, $h_0 = 1$, is an absolutely summable sequence for which $\sum_{\tau=-\infty}^{\infty} |\tau| |h_{\tau}| < \infty$ holds, $\{\varepsilon_t\}$ is a sequence of independent and identically distributed (i.i.d.) random variates with mean zero and unit variance, satisfying $E[\varepsilon_t^4] < \infty$, and σ is a positive constant. The model assumption of Eq. (1) is rather restrictive for real-life signal processing applications, but necessary in order to ensure the validity of some inference results we report in the sequel. With one exception, the signals used in the simulations of Section 5 follow the model in Eq. (1), while

the knock data experiment discussed in Section 6 deviates from the assumed model.

Let X_t , $t \in \mathbb{Z}$, have spectral density

$$C_{XX}(\omega) = \frac{1}{2\pi} \sum_{\tau=-\infty}^{\infty} c_{XX}(\tau) e^{-j\omega\tau}, \quad -\pi < \omega < \pi, \quad (2)$$

where $c_{XX}(\tau) = E[X_0 X_{|\tau|}]$, $\tau \in \mathbb{Z}$, is the covariance function of X_t , $t \in \mathbb{Z}$. Given observations x_1, \dots, x_T of the process X_t , $t \in \mathbb{Z}$, which are modelled by the random variates X_1, \dots, X_T , we construct an estimator of $C_{XX}(\omega)$, given by

$$\hat{C}_{XX}(\omega; h) = \frac{1}{T \cdot h} \sum_{k=-N}^N K\left(\frac{\omega - \omega_k}{h}\right) I_{XX}(\omega_k), \quad (3)$$

where the kernel function $K(\cdot)$ is a known symmetric, non-negative, real-valued function, h is its bandwidth and N denotes the largest integer less than or equal to $T/2$. In Eq. (3), $I_{XX}(\omega_k)$ denotes the periodogram at frequencies $\omega_k = 2\pi k/T$, $-N \leq k \leq N$, and is defined as

$$I_{XX}(\omega) = \frac{1}{2\pi T} \left| \sum_{t=1}^T X_t e^{-j\omega t} \right|^2, \quad -\pi \leq \omega \leq \pi, \quad (4)$$

E-mail address: zoubir@spg.tu-darmstadt.de

which is known to be an asymptotically unbiased, but not a consistent estimator of the spectral density $C_{XX}(\omega)$, i.e., under certain assumptions on the moment structure of ε_t and the rate of decrease of the filter coefficients $\{h_t\}, t \in \mathbb{Z}$, in Eq. (1) (see [15]), we have

$$\mathbb{E}[I_{XX}(\omega_k)] = C_{XX}(\omega_k) + O(T^{-1}), \quad (5)$$

and

$$\text{Cov}[I_{XX}(\omega_j), I_{XX}(\omega_k)] = \begin{cases} C_{XX}(\omega_j)^2 + O(T^{-1}), & j=k, \\ \frac{1}{T} C_{XX}(\omega_j) C_{XX}(\omega_k) \left(\frac{\mathbb{E}[\varepsilon_t^4]}{\sigma^4} - 3 \right) + o(T^{-1}), & j \neq k. \end{cases} \quad (6)$$

There are two main approaches for bootstrapping spectra. One could use time domain methods, wherein the resampling is performed in the time domain, followed by a computation of the resamples based bootstrap periodogram, $I_{XX}^*(\omega)$. Subsequently, the bootstrap spectral estimate $\hat{C}_{XX}^*(\omega)$ is obtained via kernel spectral density estimation as in Eq. (3), but with $I_{XX}^*(\omega_k)$ substituting the periodogram $I_{XX}(\omega_k)$ for $k = -N, \dots, N$.

Alternatively, one could use frequency domain approaches, in which the periodogram itself is resampled. These methods have attracted much attention in recent years [10] as they rely on simpler independent data resampling schemes, which are justified by the fact that periodogram ordinates at frequencies $\omega_k = 2\pi k/T$, $k = 0, 1, 2, \dots, N$, are nearly independent.

Another attractive approach, proposed recently by Kreiß and Paparoditis [8], called the autoregressive-aided periodogram bootstrap, is a combination of a parametric time domain and a non-parametric frequency domain bootstrap technique and is described in Section 4.

The objective of this paper is to compare three methods for confidence interval estimation for spectra when the sample size is small and no distributional assumptions of the data are made. We shall consider the well-established frequency domain residual based method as a “benchmark” and assess if improvements are achieved when using the tapered block bootstrap [12] or the autoregressive-aided periodogram bootstrap [8]. Results of an application of the techniques to knock data in spark ignition engines are presented.

An outline of the paper follows. First, we briefly revisit the frequency domain residual based method for bootstrapping spectra. Section 3 is an overview of a time domain bootstrap approach, the tapered block bootstrap, followed by Section 4 wherein the autoregressive-aided bootstrap is introduced. Section 5 concerns a simulation study in view of performance of the three techniques. Section 6 is an application of the presented techniques to knock data, followed by a discussion and conclusions section.

2. Frequency domain residual based bootstrap

Franke and Härdle [6], without resorting to the Gaussian assumption for X_t , $t \in \mathbb{Z}$, proposed to express the relationship between the periodogram and the spectral density as a multiplicative regression and to bootstrap the so-obtained frequency domain residuals.

The method which has been shown to be asymptotically valid is summarized below.

First, interpret the spectral estimator as the approximate multiplicative regression

$$I_{XX}(\omega_k) = C_{XX}(\omega_k) \cdot \varepsilon_k, \quad k = 1, \dots, N, \quad (7)$$

where ε_k are the residuals given by

$$\varepsilon_k = \frac{I_{XX}(\omega_k)}{C_{XX}(\omega_k)}, \quad C_{XX}(\omega_k) > 0, \quad k = 1, \dots, N. \quad (8)$$

These real valued residuals ε_k are approximately i.i.d. for N sufficiently large. To set up a confidence interval for $C_{XX}(\omega)$, proceed as depicted in Table 1 (see [6] for details).

The rescaling of residuals performed in Step 3 serves essentially the same purpose as re-centering the data in an additive regression model in order to avoid an additional bias at the resampling stage. It should also be noted that the bootstrap algorithm given in Table 1 uses three distinct kernel bandwidths, namely, an initial bandwidth h_i , a resampling bandwidth g and finally h , which may or may not be one and the same. The choice of bandwidth in kernel spectral density estimation is a crucial issue and some guidelines exist in the literature, see for example [16]. Also, the bootstrap can be successfully applied to bandwidth selection [19,2], but is not

Table 1

The residual based bootstrap procedure.

Step 1.	<i>Centering.</i> Center X_1, \dots, X_T by subtracting the sample mean.
Step 2.	<i>Initial Estimate.</i> Compute the periodogram according to Eq. (4). With an initial bandwidth $h_i > 0$, calculate $\hat{C}_{XX}(\omega; h_i)$ according to Eq. (3).
Step 3.	<i>Compute and Rescale Residuals.</i> Calculate the residuals and rescale them to obtain
	$\hat{\varepsilon}_k = \frac{I_{XX}(\omega_k)}{\hat{C}_{XX}(\omega_k; h_i)}, \quad k = 1, \dots, N$
	and rescale them to obtain
	$\tilde{\varepsilon}_k = \frac{\hat{\varepsilon}_k}{\bar{\varepsilon}}, \quad k = 1, \dots, N, \quad \bar{\varepsilon} = \frac{1}{N} \sum_{k=1}^N \hat{\varepsilon}_k.$
Step 4.	<i>Bootstrap Residuals.</i> Draw independent bootstrap residuals $\tilde{\varepsilon}_1^*, \dots, \tilde{\varepsilon}_N^*$ from $\tilde{\varepsilon}_1, \dots, \tilde{\varepsilon}_N$.
Step 5.	<i>Bootstrap Estimate.</i> Choose a resampling kernel bandwidth g and define the bootstrap periodogram as
	$I_{XX}^*(\omega_k) = I_{XX}^*(-\omega_k) = \hat{C}_{XX}(\omega_k; g) \tilde{\varepsilon}_k^*$,
	setting $I_{XX}^*(0) = 0$. Then find the bootstrap kernel spectral density estimate
	$\hat{C}_{XX}^*(\omega; h; g) = \frac{1}{T \cdot h} \sum_{k=-N}^N K\left(\frac{\omega - \omega_k}{h}\right) I_{XX}^*(\omega_k).$
Step 6.	<i>Repetition.</i> Repeat Steps 4 and 5 a large number of times.
Step 7.	<i>Confidence Interval Estimation.</i> With an arbitrary α find c_U^* such that
	$\text{Prob}^*\left(\sqrt{T \cdot h} \frac{\hat{C}_{XX}^*(\omega; h; g) - \hat{C}_{XX}(\omega; g)}{\hat{C}_{XX}(\omega; g)} \leq c_U^*\right) = \frac{\alpha}{2}$
	and set the upper bound of the $100(1-\alpha)\%$ confidence interval for $C_{XX}(\omega)$ as $\hat{C}_{XX}(\omega; h)/(1 + c_U^*(T \cdot h)^{-1/2})$. Herein, $\text{Prob}^*(\cdot)$ denotes probability conditioned on the measured data. Analogously using a c_L^* , compute the lower bound of the confidence interval.

investigated further. In the simulations given below, we fixed all bandwidths to one empirically chosen value, discussed in Section 5.

An alternative idea to bootstrapping the periodogram has been proposed by Paparoditis and Politis [11]. The method uses smoothness properties of the spectral density $C_{XX}(\omega)$ and bootstrap samples are obtained via local resampling from adjacent periodogram ordinates. Similarly to the method of Franke and Härdle [6], Paparoditis and Politis [11] explore the asymptotic independence of periodogram ordinates, but their method has the advantage of not requiring the computation of an initial spectral density estimate to obtain frequency domain residuals.

3. The tapered block bootstrap

Alternatively to Section 2, we could draw resamples in the time domain which are then used to compute the periodogram, followed by a computation of the bootstrap spectral density estimate. We shall not assume that the random variables X_1, \dots, X_T are i.i.d., but we require weak dependence of the data. The assumption of a linear process as given in Eq. (1) plays a key role in dependent data resampling and the reader is referred to [13], for example, for more details.

The most common approach to bootstrapping dependent data is block resampling. The block bootstrap methodology attempts to preserve the original time series structure by drawing blocks of a certain length with replacement from the original sample and concatenating them to generate pseudo-data [9]. The idea of a recently proposed method by Paparoditis and Politis [12], known as the *tapered block bootstrap*, is to assign different weights to the data points according to their position within their block, specifically, giving reduced weight to data near the endpoints of the window as is the case in non-parametric spectrum estimation [3,15]. Künsch's *block bootstrap* [9], which assigns equal weights to the data is a special case of the tapered block bootstrap. Tapering the block bootstrap results in a bias correction of the block bootstrap of Künsch [9] while preserving the property of asymptotic validity of the method for estimating the sampling distribution of the sample mean, provided the tapering window satisfies some regularity conditions discussed in [12]. We shall use this time domain bootstrap method for estimating confidence intervals for spectra and proceed as shown in Table 2.

Note that in Table 2, the parameter l is not equivalent to T , i.e. if the total length of the pseudo-series generated by concatenating k blocks, each of length b , is not equal to the length of the observed data sample T , one has to concatenate $k+1$ blocks and truncate the so obtained sequence to get T samples. Further, Paparoditis and Politis [12] suggest the following trapezoidal (continuous-time) function as a tapering window in Step 4,

$$w_c(\tilde{t}) = \begin{cases} \tilde{t}/c & \text{if } \tilde{t} \in [0, c], \\ 1 & \text{if } \tilde{t} \in [c, 1-c], \\ (1-\tilde{t})c & \text{if } \tilde{t} \in [1-c, 1], \end{cases} \quad (9)$$

Table 2
The tapered block bootstrap procedure.

Step 1.	Centering. Center X_1, \dots, X_T by removing the sample mean.
Step 2.	<i>Spectrum Estimation.</i> Calculate the periodogram $I_{XX}(\omega_k)$ from X_1, \dots, X_T according to Eq. (4) and the corresponding kernel spectral density estimate $\hat{C}_{XX}(\omega_k)$, $k = 1, \dots, N$, as in Eq. (3).
Step 3.	<i>Set the Bootstrap Parameters.</i> Choose a block size b , where b is a positive integer less than T and define $k = \lfloor T/b \rfloor$ as the number of blocks to draw from, where $\lfloor \cdot \rfloor$ denotes the integer part.
Step 4.	<i>Draw Bootstrap Resamples.</i> Let the integers i_0, i_1, \dots, i_{k-1} be drawn independently and identically distributed with distribution uniform on the set $\{1, 2, \dots, T-b+1\}$. Then for $m = 0, 1, \dots, k-1$, compute
	$X_{mb+j}^* = w_b(j) \frac{\sqrt{b}}{\ w_b\ _2} X_{i_m+j-1}, \quad j = 1, 2, \dots, b,$
	which yields the pseudo-series $X_1^*, X_2^*, \dots, X_l^*$ of size $l = k \cdot b$. Herein w_b denotes the tapering window defined in Eq. (9) and $\ w_b\ _2 = (\sum_{t=1}^b w_b(t)^2)^{1/2}$.
Step 5.	<i>Construct Bootstrap Estimates.</i> Center the pseudo-series $X_1^*, X_2^*, \dots, X_l^*$ and find the bootstrap periodogram $I_{XX}^*(\omega_k)$ for $-N^* < k < N^*$, computed as in Eq. (4), replacing T by l and X_1, \dots, X_T by $X_1^*, X_2^*, \dots, X_l^*$, where $N^* = \lfloor l/2 \rfloor$ and $I_{XX}^*(0) = 0$. Then find the corresponding bootstrap kernel spectral density estimate $\hat{C}_{XX}^*(\omega)$ as in Eq. (3), with l replacing T .
Step 6.	<i>Repetition.</i> Repeat Steps 4 and 5 a large number of times.
Step 7.	<i>Confidence Interval Estimation.</i> Find confidence bounds as in Step 7 of Table 1, replacing T by l .

where $c = 0.43$ should be chosen so as to minimize a mean squared measure for a fixed covariance structure [12]. As is the case in non-parametric spectrum estimation, the discrete-time version of the tapering window in Eq. (9) is obtained via dilations.

In addition to the tapering window shape, selection of the block length b is crucial as it heavily affects the performance of the tapered block bootstrap in practice. The optimum block length depends on the unknown quantities $\sum_{\tau=-\infty}^{\infty} c_{XX}(\tau)$ and $\sum_{\tau=-\infty}^{\infty} \tau^2 c_{XX}(\tau)$ (see [12] for details). Given estimates of the latter quantities, one can determine an estimate of the optimum block length, which (under some regularity conditions and choosing the bandwidth M of the window used in the estimation of the above unknown quantities to be proportional to $N^{1/5}$ [12]) in the worst case achieves, with respect to the theoretical but unknown optimum length, a rate of $O_p(N^{-2/5})$ as compared to the rate of $O_p(N^{-2/7})$ achieved by the block size estimator for the (untapered) block bootstrap of Bühlmann and Künsch [4].

4. The autoregressive-aided periodogram bootstrap

The idea of Kreiß and Paparoditis [8] of combining a time domain and a frequency domain bootstrap approach for spectral densities is to generate, via the parametric fit, periodogram ordinates that capture the essential features of the data and the weak dependence structure of the periodogram, while the non-parametric correction is to catch features not represented by the parametric fit. The

method named *autoregressive-aided periodogram bootstrap* is more general than the residual based method of **Table 1** or that of Paparoditis and Politis [11].

Let

$$\tilde{X}_t = \sum_{\tau=1}^p a_\tau \tilde{X}_{t-\tau} + \tilde{\sigma} \tilde{\varepsilon}_t, \quad (10)$$

where $\mathbf{a} = (a_1, \dots, a_p)' = \Gamma^{-1} \mathbf{c}_{\tilde{X}}$, $(\Gamma)_{i,j} = 1, 2, \dots, p = c_{\tilde{X}\tilde{X}}(i-j)$, $\mathbf{c}_{\tilde{X}} = (c_{\tilde{X}\tilde{X}}(1), c_{\tilde{X}\tilde{X}}(2), \dots, c_{\tilde{X}\tilde{X}}(p))'$ and $\tilde{\varepsilon}_t$ is an i.i.d. sequence with mean zero and unit variance, and where $E[\tilde{\varepsilon}_t^4] < \infty$. The spectral density of \tilde{X}_t is given by

$$C_{\tilde{X}\tilde{X}}(\omega) = \frac{\tilde{\sigma}^2}{|1 - \sum_{\tau=1}^p a_\tau e^{-j\omega\tau}|^2}, \quad (11)$$

with $\tilde{\sigma}^2 = c_{\tilde{X}\tilde{X}}(0) - \mathbf{a}' \Gamma^{-1} \mathbf{a}$.

Consider now the random variables

$$I_{YY}(\omega_k) = q(\omega_k) I_{\tilde{X}\tilde{X}}(\omega_k), \quad \omega_k = \frac{2\pi k}{T}, \quad k = -N, \dots, N, \quad (12)$$

where

$$q(\omega) = \frac{C_{XX}(\omega)}{C_{\tilde{X}\tilde{X}}(\omega)} \quad (13)$$

and

$$I_{\tilde{X}\tilde{X}}(\omega) = \frac{1}{2\pi T} \left| \sum_{t=1}^T \tilde{X}_t e^{-j\omega t} \right|^2, \quad -\pi \leq \omega \leq \pi, \quad (14)$$

the periodogram based on $\tilde{X}_1, \tilde{X}_2, \dots, \tilde{X}_T$ from \tilde{X}_t , $t \in \mathbb{Z}$. From the definition of $q(\omega)$, clearly,

$$E[I_{YY}(\omega_k)] = C_{XX}(\omega_k) + O(T^{-1}) \quad (15)$$

and

$$\text{Cov}[I_{YY}(\omega_j), I_{YY}(\omega_k)] = \begin{cases} C_{XX}(\omega_j)^2 + O(T^{-1}), & j = k, \\ \frac{1}{T} C_{XX}(\omega_j) C_{XX}(\omega_k) \left(\frac{E[\tilde{\varepsilon}_t^4]}{\tilde{\sigma}^4} - 3 \right) + o(T^{-1}), & j \neq k, \end{cases} \quad (16)$$

holds since Eqs. (5) and (6) are satisfied for $I_{\tilde{X}\tilde{X}}(\omega)$ with $C_{XX}(\omega)$ replaced by $C_{\tilde{X}\tilde{X}}(\omega)$ and $E[\tilde{\varepsilon}_t^4]/\sigma^4$ replaced by $E[\tilde{\varepsilon}_t^4]/\tilde{\sigma}^4$. Furthermore, the periodogram ordinates $I_{YY}(\omega_s)$, $s = 1, \dots, m$, for frequencies $0 < \omega_1 < \omega_2 < \dots < \omega_m < \pi$ are independently distributed as χ_2^2 variates with mean $C_{XX}(\omega_s)$ and variance $C_{XX}(\omega_s)^2$, as is the case for the ordinary periodogram, provided $C_{XX}(\omega) > 0$ for $\omega \in [0, \pi]$. Since the random variables $I_{YY}(\omega_s)$, $s = 1, \dots, m$, resample closely the random behavior of the periodogram ordinates $I_{XX}(\omega_s)$, the above results suggest that the distribution of a statistic based on $I_{XX}(\omega_s)$ can be well approximated by the corresponding statistic based on $I_{YY}(\omega_s)$. Furthermore, if $E[\tilde{\varepsilon}_t^4]/\tilde{\sigma}^4$ is close to $E[\tilde{\varepsilon}_t^4]/\sigma^4$, the approximation will also be valid for periodogram statistics for which the dependence of the periodogram ordinates affects the asymptotic distribution of interest [8]. This is expected to be true in this case because the covariance structure in Eq. (16) mimics that of Eq. (6).

The key idea of the autoregressive-aided periodogram bootstrap is to combine a parametric autoregressive approximation of X_t , $t \in \mathbb{Z}$, given X_1, X_2, \dots, X_T , with a non-parametric “correction” function $q(\cdot)$ to resample the stochastic behavior of $I_{XX}(\omega)$. However, it is not necessary

to use an autoregressive model for the parametric part. Alternatively, one could approximate the time series by a moving average process [8], which is not further investigated here. The procedure of the autoregressive-aided periodogram bootstrap is summarized in **Table 3**.

In the autoregressive-aided periodogram bootstrap method of **Table 3**, we perform two smoothing operations with a kernel function $K(\cdot)$, which we choose to be the Bartlett-Priestley kernel [15, p. 444]. On one hand, $q(\omega)$ is estimated via smoothing $I_{XX}(\omega_k)/\hat{C}_{\tilde{X}\tilde{X}}(\omega_k)$ and on the other hand, $I_{XX}^*(\omega_k)$ is smoothed to obtain $\hat{C}_{\tilde{X}\tilde{X}}^*(\omega)$. As to the bandwidth h , we followed Kreiß and Paparoditis [8] who suggest a leave-one-out kernel estimator for $q(\omega)$ which is obtained by deleting one periodogram ordinate. Then, for a given p and $\hat{C}_{\tilde{X}\tilde{X}}(\omega)$, h is found as the minimizer of Beltrão and Bloomfield's [1] discretized version of Whittle's approximation of minus twice the Gaussian likelihood, given by

$$\sum_{k=1}^N \left\{ \log C_{XX}(\omega_k) + \frac{I_{XX}(\omega_k)}{C_{XX}(\omega_k)} \right\},$$

but substituting $q(\omega_k)\hat{C}_{\tilde{X}\tilde{X}}(\omega_k)$ for $C_{XX}(\omega_k)$, the leave-one-out estimate of $q(\omega_k)$ for $q(\omega_k)$ and $\hat{C}_{\tilde{X}\tilde{X}}(\omega_k)$ for $C_{\tilde{X}\tilde{X}}(\omega_k)$.

Table 3
The autoregressive-aided periodogram bootstrap procedure.

Step 1.	Estimate the Spectrum. Fit an autoregressive process of order p to X_1, \dots, X_T , compute consistent estimators $\hat{a}_1, \dots, \hat{a}_p, \hat{\sigma}^2$ and $\hat{C}_{\tilde{X}\tilde{X}}(\omega) = \hat{\sigma}^2 1 - \sum_{\tau=1}^p \hat{a}_\tau e^{-j\omega\tau} ^{-2}$, $0 \leq \omega \leq \pi$.
Step 2.	Estimate $q(\omega)$. With a kernel function $K(\cdot)$ and a properly chosen bandwidth $h > 0$, compute
	$\hat{q}(\omega) = \frac{1}{T \cdot h} \sum_{k=-N}^N K\left(\frac{\omega - \omega_k}{h}\right) \frac{I_{XX}(\omega_k)}{\hat{C}_{\tilde{X}\tilde{X}}(\omega_k)}, \quad 0 \leq \omega < \pi.$
Step 3.	Compute Residuals. Compute the residuals
	$\hat{\varepsilon}_t = X_t - \sum_{\tau=1}^p \hat{a}_\tau X_{t-\tau}, \quad t = p+1, \dots, T$
	and standardize them in order to get an empirical distribution with mean zero and unit variance.
Step 4.	Resampling. Generate a sequence of i.i.d. resamples $\{\hat{\varepsilon}_t^*\}$ and $X_1^*, X_2^*, \dots, X_T^*$, according to
	$X_t^* = \sum_{\tau=1}^p \hat{a}_\tau X_{t-\tau}^* + \hat{\sigma} \cdot \hat{\varepsilon}_t^*.$
Step 5.	Compute the Pseudo-Periodogram. Compute the periodogram of the bootstrap observations,
	$I_{XX}^*(\omega) = \frac{1}{2\pi T} \left \sum_{t=1}^T X_t^* e^{-j\omega t} \right ^2, \quad 0 \leq \omega \leq \pi.$
Step 6.	Compute the Bootstrap Spectral Density. Compute the bootstrap periodogram
	$I_{XX}^*(\omega) = \hat{q}(\omega) I_{XX}^*(\omega), \quad 0 \leq \omega \leq \pi.$
	and the corresponding kernel spectral density estimate $\hat{C}_{\tilde{X}\tilde{X}}^*(\omega)$, $0 \leq \omega \leq \pi$.
Step 7.	Repetition. Repeat Steps 4–6 a large number of times.
Step 8.	Estimate Confidence Interval. Find confidence bounds as in Step 7 of Table 1 , replacing $\hat{C}_{XX}(\omega)$ by $\hat{q}(\omega) \cdot \hat{C}_{\tilde{X}\tilde{X}}(\omega)$.

The non-parametric frequency domain residual based periodogram bootstrap differs from the autoregressive-aided periodogram bootstrap not only by the independence of the generated bootstrap periodogram ordinates $J_{XX}^*(\omega_k)$ but also by the estimator of the spectral density $C_{XX}(\omega)$ used. In particular, the kernel estimator $\hat{C}_{XX}(\omega)$ is replaced by the estimator $\tilde{C}_{XX} = \hat{q}(\omega) \cdot \hat{C}_{\tilde{X}\tilde{X}}(\omega)$ in the autoregressive-aided bootstrap. The latter estimator is uniformly bootstrap. The latter estimator is uniformly consistent for every p fixed, i.e., (see [8] for more details),

$$\sup_{\omega \in [0, \pi]} |\tilde{C}_{XX}(\omega) - C_{XX}(\omega)| \rightarrow 0 \text{ in prob.}$$

5. A simulation study

We present a simulation study which illustrates the performance of the methods discussed in the preceding sections. We used the two models from [22], namely

Model 1:

$$X_t = 0.5X_{t-1} - 0.6X_{t-2} + 0.3X_{t-3} - 0.4X_{t-4} + 0.2X_{t-5} + N_t,$$

where N_t are independent standard normal variables.

Model 2:

$$X_t = X_{t-1} - 0.7X_{t-2} - 0.4X_{t-3} + 0.6X_{t-4} - 0.5X_{t-5} + U_t,$$

where U_t are independently and uniformly distributed variables on the interval $[-2.5, 2.5]$, with a sample size of $T = 256$. For all methods, we used the Bartlett-Priestley kernel function [15, p. 444] with a bandwidth of $h_i = g = h = 0.05$ for Model 1 and $h_i = g = h = 0.03$ for Model 2.

Knowing that Models 1 and 2 are autoregressive processes, we also applied a bootstrap technique for autoregressive processes (see [17], for example). However, we did not assume p to be known, but we estimated p as in the autoregressive-aided periodogram bootstrap (see above).

A reasonable block size for the tapered block bootstrap was obtained by manually inspecting $\hat{c}_{XX}(\tau)$ to find the smallest integer τ after which the covariance appears

negligible. Specifically, we used $b = 38$ and 71 for Models 1 and 2, respectively.

Note also that in Table 3 the model order p is assumed to be known. In practice, model order selection has to be performed to get an estimate \hat{p} of p . The order of the autoregressive process was estimated using Akaike's criterion, which minimizes $AIC(p) = \arg \min_p \{\hat{\sigma}^2(1+2p/T)\}$ over a range of values $p = 1, 2, \dots, p_{\max}(T)$. Such a choice of p leads to an asymptotically optimal autoregressive spectral estimator $\hat{C}_{\tilde{X}\tilde{X}}(\omega)$ in the sense of minimizing the relative squared error $\int_{-\pi}^{\pi} ((\hat{C}_{\tilde{X}\tilde{X}}(\omega) - C_{XX}(\omega))/C_{XX}(\omega))^2 d\omega$, see, for example, [18].

The confidence interval approximations are based on 1000 bootstrap resamples and averaged over 1000 Monte Carlo runs. First, we show results for Model 1. Fig. 1 displays the confidence bounds when using a time domain residual based approach for autoregressive processes. In comparison, we also show in Fig. 1 the result of confidence interval estimation for the same model, but with the frequency domain residual based bootstrap method of Franke and Härdle [6], described in Table 1. It is clearly seen that the confidence bounds based on the time domain residual based bootstrap for autoregressive processes are tighter than those obtained with the frequency domain residual based bootstrap method, which was expected. Tighter bounds than those reached with the frequency domain residual based method are obtained with the autoregressive-aided periodogram bootstrap of Table 3 as shown in Fig. 2, but they remain larger than those obtained with the time domain residual based bootstrap for autoregressive processes. If we apply the tapered block bootstrap of Table 2, then we obtain the result depicted in Fig. 3, which is slightly worse than that of Fig. 1. Similar results are obtained with Model 2, where it was found that the autoregressive-aided periodogram bootstrap achieved the best results compared to the frequency domain residual based bootstrap or the tapered block bootstrap. In Fig. 4, the estimated confidence bounds obtained with the autoregressive-aided periodogram bootstrap are compared with those resulting from the

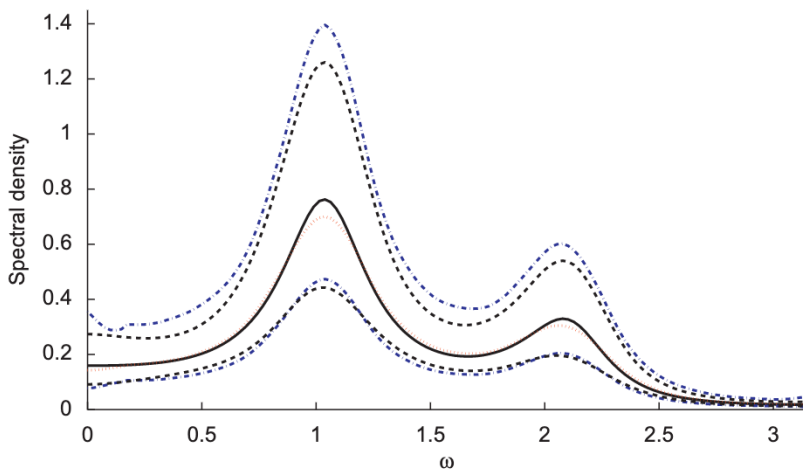


Fig. 1. Estimate of an 95% confidence interval for the spectral density of Model 1 obtained with the frequency domain residual based method of Franke and Härdle [6] (dashed-dotted line). The result of a time domain approach based on bootstrapping residuals of an autoregressive process is also shown (dashed line). The solid line is the true spectral density while the dotted line is its kernel estimate.

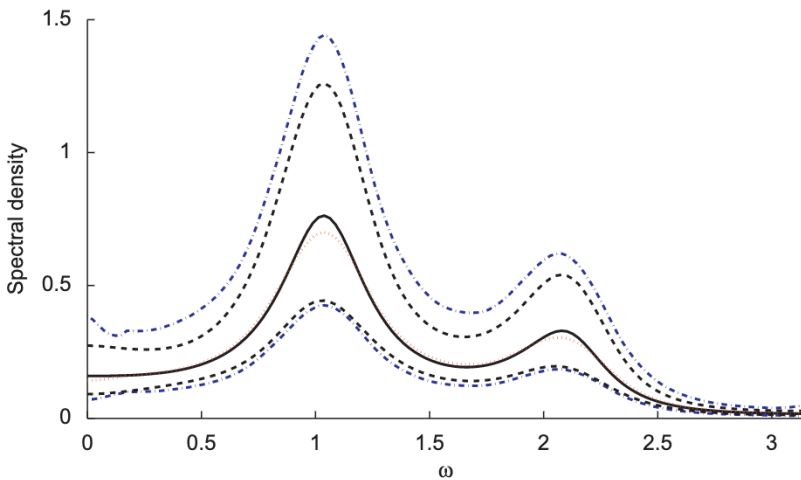


Fig. 2. Estimate of an 95% confidence interval for the spectral density of Model 1 obtained with the autoregressive-aided periodogram bootstrap of Kreiß and Paparoditis [8] (dashed-dotted line). The result of a time domain approach based on bootstrapping residuals of an autoregressive process is also shown (dashed line). The solid line is the true spectral density while the dotted line is its kernel estimate.

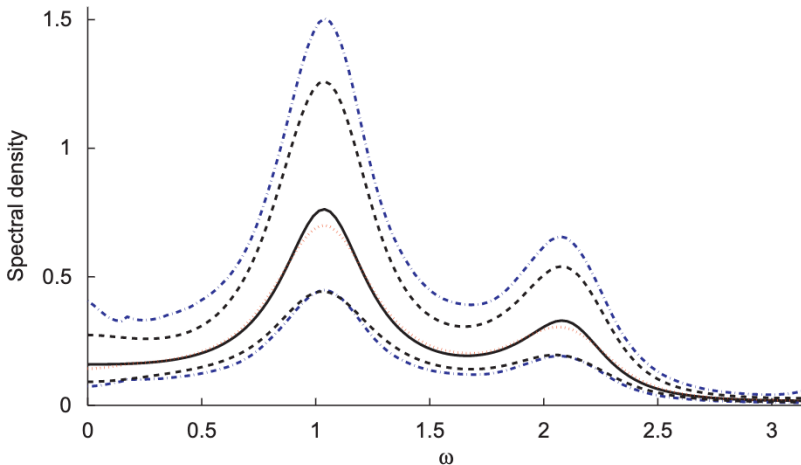


Fig. 3. Estimate of an 95% confidence interval for the spectral density of Model 1 obtained with the time domain based tapered block bootstrap of Paparoditis and Politis [12] (dashed-dotted line). The result of a time domain approach based on bootstrapping residuals of an autoregressive process is also shown (dashed line). The solid line is the true spectral density while the dotted line is its kernel estimate.

time domain residual based bootstrap for autoregressive processes.

A quantitative comparison of the discussed method based on estimates of coverage probabilities at certain frequency bins, $\omega_k = 2\pi k/T$ was conducted for all methods. For Model 1 the considered frequency bins correspond to two peaks and the through between both peaks (see the solid line of Fig. 1). For Model 2, the chosen frequency bins in Table 5 correspond to two peaks and the minimum of the true spectral density (see the solid line of Fig. 4). The confidence interval results are shown in Tables 4 and 5 for Models 1 and 2, respectively. We also applied the (untapered) block bootstrap of Künsch [9], not shown here, but the estimated coverage was lower than the one obtained with the tapered block bootstrap which confirms the presence of a larger bias.

From Table 4, one can clearly see that the time domain residual based bootstrap for an autoregressive model achieves among all methods the best results. This is not necessarily true in Table 5 (see column 4) for Model 2. As one can observe, the confidence interval obtained with the autoregressive-aided periodogram bootstrap achieves slightly better results and the method is thus competitive. There is a pronounced drop in performance when applying the tapered block bootstrap to Model 2 at the given frequencies (see column 3 in Table 5). It should be recalled that the tapered block bootstrap is sensitive to the block length and the suggested guidelines by Paparoditis and Politis [12] seem to work well under some conditions only, such as Gaussian data.

The frequency domain residual based method of Franke and Härdle [6] seems to perform reasonably well,

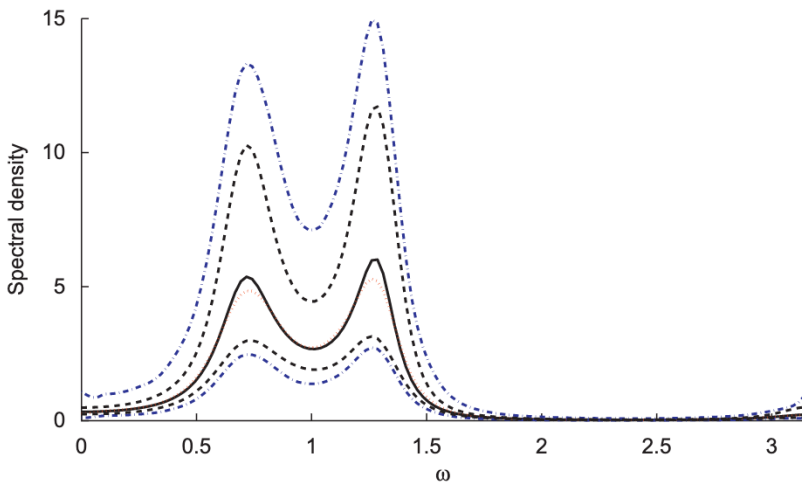


Fig. 4. Estimate of an 95% confidence interval for the spectral density of Model 2 obtained with the autoregressive-aided periodogram bootstrap of Kreiß and Paparoditis [8] (dashed-dotted line). The result of a time domain approach based on bootstrapping residuals of an autoregressive process is also shown (dashed line). The solid line is the true spectral density while the dotted line is its kernel estimate.

Table 4

Estimates of coverage probabilities in (%) of a nominal 95% confidence interval obtained with the frequency domain residual based bootstrap (RSD) of Table 1, the tapered block bootstrap (TBB) of Table 2, the time domain residual based bootstrap (AR) and the autoregressive-aided periodogram bootstrap (AR-AP) of Table 3 for Model 1 with Gaussian innovations.

k	RSD	TBB	AR	AR-AP
41	85.91	84.56	91.69	88.65
42	85.24	83.97	91.65	88.31
43	84.93	83.60	91.59	88.20
66	89.30	84.00	92.90	89.84
67	89.55	84.21	92.95	89.96
68	88.78	83.43	92.98	89.52
83	86.95	85.20	92.01	89.10
84	86.39	85.21	91.91	89.01
85	85.84	84.95	91.87	88.77

Table 5

Estimates of coverage probabilities in (%) of a nominal 95% confidence interval obtained with the frequency domain residual based bootstrap (RSD) of Table 1, the tapered block bootstrap (TBB) of Table 2, the time domain residual based bootstrap (AR) and the autoregressive-aided periodogram bootstrap (AR-AP) of Table 3 for Model 2 with uniformly distributed innovations on $[-2.5, 2.5]$.

k	RSD	TBB	AR	AR-AP
26	86.68	77.98	87.66	88.27
27	85.94	77.55	87.54	87.85
28	85.64	77.77	87.62	87.96
52	84.08	78.48	85.76	87.60
53	83.61	77.80	85.88	87.43
54	84.30	77.88	86.44	87.56
95	86.73	76.74	87.72	90.31
96	87.52	77.41	87.78	90.80
97	87.80	77.98	87.85	91.32

but the results depend on the underlying frequency bins and the distribution of the data. This could be due to the assumption of independent periodogram ordinates, which

is not necessarily given for the sample size used here. Similar results were obtained for different distributions of the innovations.

It is worth noting that while the autoregressive-aided periodogram bootstrap procedure uses explicitly an autoregressive model, neither the frequency domain residual based bootstrap of Franke and Härdle nor the tapered block bootstrap of Paparoditis and Politis use resamples from residuals of an autoregressive model. Therefore, the signal models 1 and 2 used in the simulation study are favorable for the method of Kreiß and Paparoditis [8]. However, recall that the autoregressive-aided periodogram bootstrap allows for an alternate (linear process) model, not necessarily an autoregressive model. In order to assess the performance of the discussed methods, in particular the autoregressive-aided periodogram bootstrap in view of the model choice, we used a moving average process of order 1 (MA(1)) as well as a non-linear model described below because these models are not well approximated in finite sample situations by autoregressive models. We consider the following models

Model 3:

$$X_t = Z_t + 0.99Z_{t-1},$$

Model 4:

$$X_t = 0.5X_{t-1}\exp(-X_{t-1}^2/4) + Z_t,$$

where in both cases Z_t are independent standard normal variates.

The simulation settings for Models 3 and 4 are similar to the ones for Models 1 and 2, except that we used a block size of $b = 9$ and 12 for the MA(1) process and the non-linear process, respectively. Fig. 5 displays the confidence bounds obtained using the frequency domain residual based bootstrap method of Franke and Härdle [6], along with the results obtained with the autoregressive-aided periodogram bootstrap of Table 3 as well as the tapered block bootstrap of Table 2. Except for the tapered block bootstrap at some low frequency bins, the results

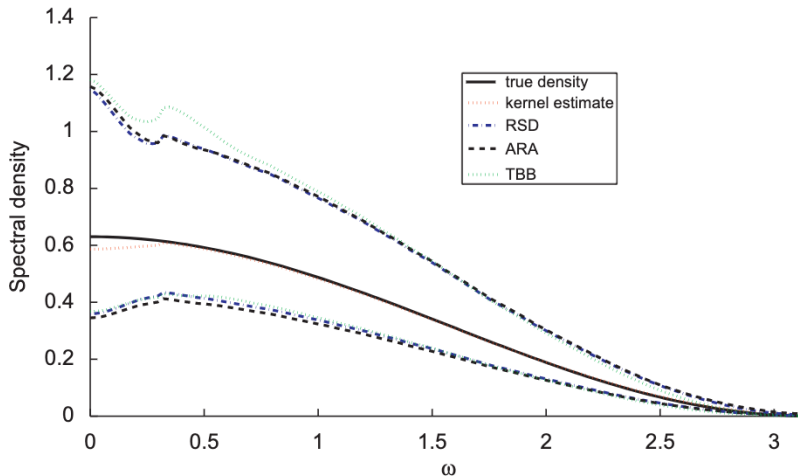


Fig. 5. Estimates of an 95% confidence interval for the spectral density of Model 3 obtained with the time domain based tapered block bootstrap of Paparoditis and Politis [12] (dotted line). The results obtained with the autoregressive-aided periodogram bootstrap of Kreiß and Paparoditis [8] (dashed line) and the frequency domain residual based method of Franke and Härdle [6] (dashed-dotted line) are also shown. The solid line is the true spectral density while the dotted line is its kernel estimate.

Table 6

Estimates of coverage probabilities in (%) of a nominal 95% confidence interval obtained with the frequency domain residual based bootstrap (RSD) of Table 1, the tapered block bootstrap (TBB) of Table 2 and the autoregressive-aided periodogram bootstrap (AR-AP) of Table 3 for Model 3 with standard normally distributed innovations.

k	RSD	TBB	AR-AP
5	91.53	80.01	90.62
6	91.91	81.20	90.61
7	92.21	82.63	90.45
25	90.26	75.25	89.39
26	90.24	75.28	89.43
30	90.30	76.05	89.50
88	90.17	74.57	89.25
89	90.08	73.92	89.25
90	90.18	72.94	89.38

Table 7

Estimates of coverage probabilities in (%) of a nominal 95% confidence interval obtained with the frequency domain residual based bootstrap (RSD) of Table 1, the tapered block bootstrap (TBB) of Table 2 and the autoregressive-aided periodogram bootstrap (AR-AP) of Table 3 for Model 4 with standard normally distributed innovations.

k	RSD	TBB	AR-AP
12	90.64	84.98	91.00
13	89.95	83.61	90.41
14	88.51	80.87	88.98
34	90.14	80.58	90.50
35	90.20	80.68	90.57
36	90.08	80.45	90.51
88	90.62	82.56	90.87
89	90.30	82.17	90.48
90	90.32	82.21	90.45

obtained are comparable to the previous ones. The tapered block bootstrap seems to have some difficulties with the non-linear model as it results in a large bias at low frequencies, as depicted in Fig. 6. Both the autoregressive-aided periodogram bootstrap and the frequency domain residual based bootstrap behave similarly and lead to satisfactory results.

A quantitative comparison of the results obtained for Models 3 and 4 is given by the estimated coverage probabilities of the three methods at selected frequency bins, $\omega_k = 2\pi k/T$. The confidence interval results are shown in Tables 6 and 7 for Models 3 and 4, respectively. The tables show again the superiority of the frequency domain residual method of Franke and Härdle [6] and the autoregressive-aided periodogram bootstrap of Kreiß and Paparoditis [8], which display comparable results. The tapered block bootstrap of Table 2 displays a bias in the coverage.

Considering all simulation results, it seems that overall the autoregressive-aided periodogram bootstrap technique is the most stable and the most promising method as

compared to the frequency domain residual based bootstrap or the tapered block bootstrap. In the next section, we shall discuss an application of confidence interval estimation with the autoregressive-aided periodogram bootstrap to combustion engine data for the characterization of knock.

6. Experimental analysis

The demands on today's combustion engines are ever increasing. Special interest continues to be reduction of fuel consumption due to dwindling oil reserves and to meeting the demands of new legislations on greenhouse gas emissions. A means for lowering fuel consumption in spark ignition engines is to increase the compression ratio. A further increase in compression is, however, limited by the occurrence of knock—an extremely fast combustion that generates a knocking or ringing sound.

Knock can be controlled by adapting the angle of ignition. To attain safe operation at maximum efficiency, engine control systems which detect knock and adapt

spark timing of each cylinder separately are of special interest. However, the performance of such systems suffers from the low signal-to-noise power ratio (SNR) of structure-borne sound measured by accelerometers. In-cylinder pressure is preferred because of its high SNR but it requires proper mounting of a pressure sensor in each cylinder. Corresponding costs restrict the use of in-cylinder pressure sensing to reference purposes in engine or fuel development. Although approaches to reconstruct cylinder-wise pressure have been proposed in the literature (see, for example [7] and references therein), we shall also make use of in-cylinder pressure measurements (Fig. 7).

The data we used was collected at ROBERT BOSCH GMBH on an engine testbed. Measurements of in-cylinder pressure as well as structure-borne sound from a combustion engine running at 3500 rpm under knocking

conditions were recorded and sampled at 100 kHz. The original data have been high-pass filtered because resonance frequencies excited by knock arise at higher frequencies. As an example, we show the time series of a pressure signal in Fig. 7 and of a structure-borne sound signal from the corresponding combustion cycle in Fig. 8. In Fig. 9, the estimated spectral densities of pressure (solid line) and structure-borne sound (dashed-dotted line), which were obtained by averaging periodograms over 594 cycles are displayed. The figure shows the four resonance frequencies excited by knock, more clearly in the spectral density of in-cylinder pressure (solid line) than of structure-borne sound (dashed-dotted line).

Because the autoregressive-aided periodogram bootstrap performed best in simulations, we shall show results based on this method only. It is obvious that due to the non-stationary nature of knock signals [5] some condi-

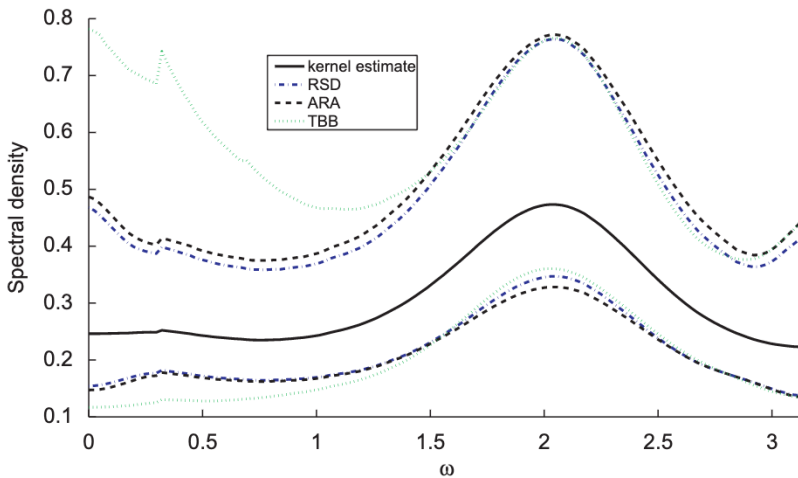


Fig. 6. Estimates of an 95% confidence interval for the spectral density of Model 4 obtained with the time domain based tapered block bootstrap of Paparoditis and Politis [12] (dotted line). The results obtained with the autoregressive-aided periodogram bootstrap of Kreiß and Paparoditis [8] (dashed line) and the frequency domain residual based method of Franke and Härdle [6] (dashed-dotted line) are also shown. The solid line is a kernel spectral density estimate of the true but unknown spectral density.

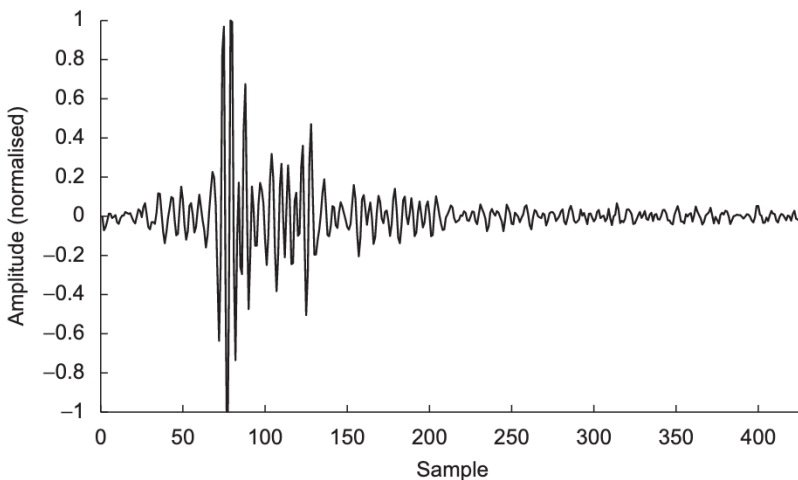


Fig. 7. In-cylinder pressure signal (high-pass filtered) of a knocking combustion cycle.

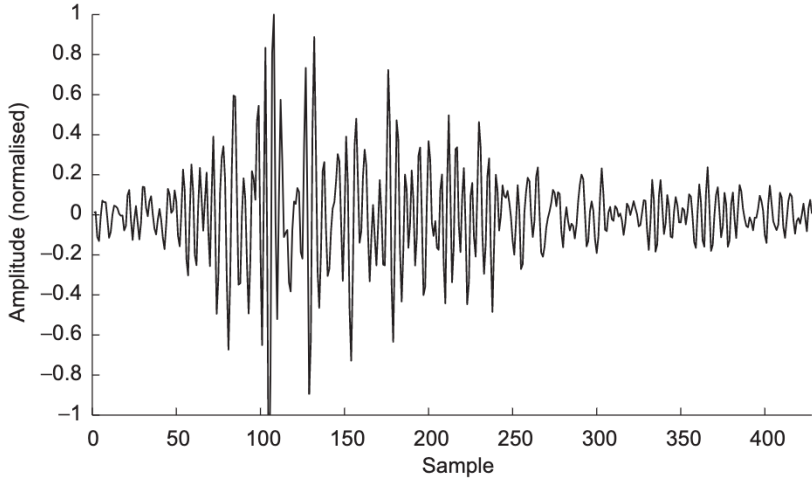


Fig. 8. Structure-borne sound signal of a knocking combustion cycle.

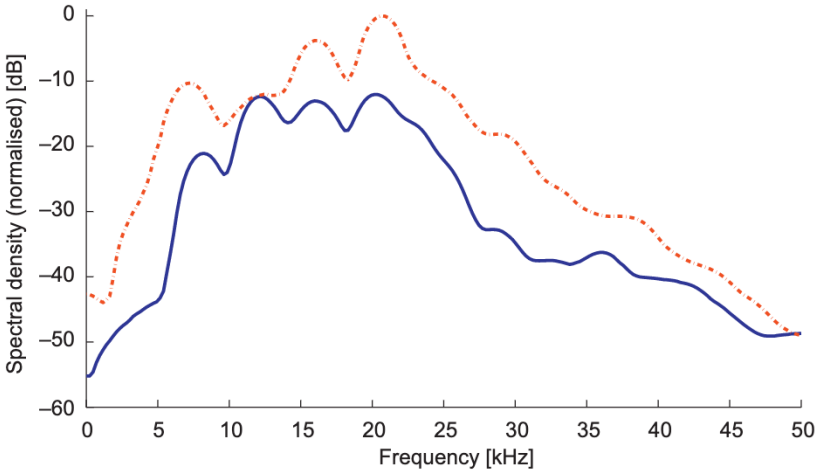


Fig. 9. Spectral density estimates for in-cylinder pressure (solid) and structure-borne sound (dashed-dotted) obtained by averaging 594 periodograms.

tions for the validity of the bootstrap method such as the assumption of a linear process in Eq. (1) are not fulfilled. However, we observed that similar confidence intervals for spectral densities are obtained when bootstrapping over independent cycles (multiple realizations), which confirms the robustness of the autoregressive-aided bootstrap in practice.

In Figs. 10 and 11, we show the confidence bounds obtained with the method of Table 3. Confidence bounds are quite important for the application as detecting knock is usually performed by measuring the power at the resonance modes and deciding for a knocking cycle when the latter is too large. There is a well known and established duality between confidence intervals and hypothesis testing, i.e., if \mathcal{I} is a confidence interval for an unknown parameter θ , with coverage probability α , then a $(1-\alpha)$ -level test of the null hypothesis $H: \theta = \theta_0$ against $K: \theta \neq \theta_0$ is to reject H if $\theta_0 \notin \mathcal{I}$. Therefore, the estimation of confidence intervals is very helpful for the

detection of knock. The detection of knock is, however, beyond the scope of this paper. The results serve merely as examples for the applicability of bootstrap based confidence interval estimation for spectral densities of knock signals.

Another important problem in engine diagnosis is the study of the relationship between cylinder pressure $X(n)$ and structure-borne sound $Y(n)$ at a given frequency, such as the transfer function $H_{YX}(\omega) = C_{YX}(\omega)/C_{XX}(\omega)$ or the coherence function $|R_{YX}(\omega)|^2 = |C_{YX}(\omega)|^2/(C_{YY}(\omega)C_{XX}(\omega))$. These measures can be of relevance for finding suitable sensor positions for knock detection [21]. Suitably placed vibration sensors improve, independently of the knock detection scheme used, the detectability of knocking cycles. Confidence intervals and statistical tests for the coherence function play therefore an important role. Analytic results for the sample coherence function are tedious and the bootstrap overcomes this problem with more computations and less distributional assumptions,

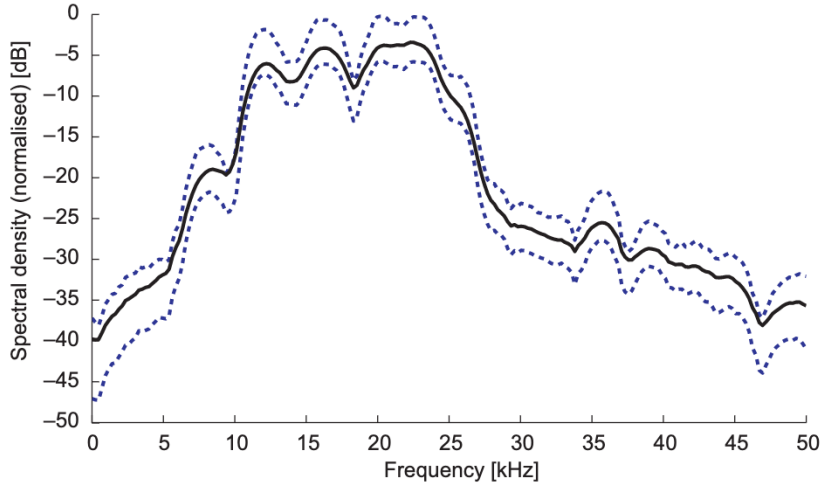


Fig. 10. Estimated 95% confidence interval (dashed line) for the spectral density of in-cylinder pressure, along with the spectral density estimate for the combustion cycle of Fig. 7.

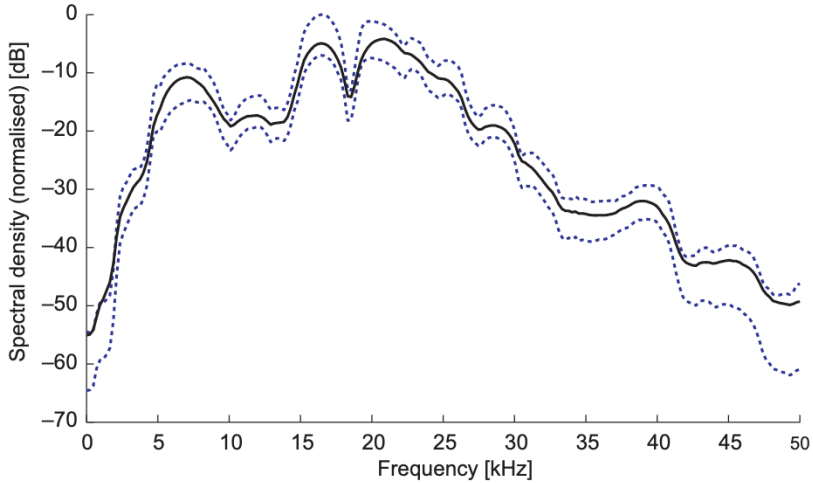


Fig. 11. Estimated 95% confidence interval for the spectral density of structure-borne sound, along with the spectral density estimate for the combustion cycle of Fig. 8.

as it was shown in [20], where we proposed a method for bootstrapping the coherence function from multiple data stretches. We could proceed similarly in this case as we have independent combustion cycles available to us and we could resample these. Based on one data stretch only, it is not straightforward to apply a frequency domain bootstrap to construct confidence intervals for cross-spectra. The application of a block bootstrap is more appropriate in this case [14]. Due to space limitations, we shall omit cross-spectral density analysis and shall report results elsewhere.

7. Discussion and conclusions

In this paper, we have discussed the estimation of confidence intervals for spectra with the bootstrap.

Specifically, we have compared a frequency domain method, a time domain method and a time domain and frequency domain combined method. We have shown simulation results such as confidence coverages for Gaussian and non-Gaussian processes. It was found that the method of Kreiß and Paparoditis, the autoregressive-aided periodogram bootstrap, which combines a time domain and a frequency domain resampling scheme performs well in that it maintains a coverage level close to the preset one. We have therefore used the technique to construct confidence intervals for spectral densities of pressure signals and structure-borne sound signals recorded on a spark ignition engine under knock conditions. Noting that the underlying real-life signals do not follow the assumed model of linear processes, the autoregressive-aided periodogram bootstrap has shown its good performance and is therefore robust.

Acknowledgements

The author wishes to thank Michael Lang for his help with the simulations and Dr. Hamedovic of ROBERT BOSCH GMBH for providing the knock data. Also, the author wishes to thank the anonymous reviewers for their constructive comments.

References

- [1] K.I. Beltrão, P. Bloomfield, Determining the bandwidth of a kernel spectrum estimate, *J. Time Ser. Anal.* 8 (1987) 21–38.
- [2] R.F. Brcic, A.M. Zoubir, Bootstrap based nonparametric curve and confidence band estimates for spectral densities, in: Proceedings of the 1st IEEE International Workshop on Computational Advances in Multi-Sensor Adaptive Processing (CAMSAP), Puerto Vallarta, Mexico, December 2005, pp. 81–84.
- [3] D.R. Brillinger, *Time Series: Data Analysis and Theory*, Holden-Day, San Francisco, 1981.
- [4] P. Bühlmann, H.R. Künsch, Block length selection in the bootstrap for time series, *Comput. Statist. Data Anal.* 31 (1999) 295–310.
- [5] S. Carstens-Behrens, J.F. Böhme, Combustion diagnosis by time-frequency analysis of pressure and structure-borne sound signals, in: B. Boashash (Ed.), *Time-Frequency Signal Analysis and Processing*, Elsevier Science Publishers, 2003, pp. 635–642.
- [6] J. Franke, W. Härdle, On bootstrapping kernel estimates, *Ann. Statist.* 20 (1992) 121–145.
- [7] C. Kallenberger, A. Nistor, H. Hamedovic, F. Raichle, J. Breuninger, W. Fischer, T. Baehren, K. Benninger, A.M. Zoubir, Estimation of cylinder-wise combustion features from engine speed and cylinder pressure, *SAE Int. J. Engines* 1 (1) (2009) 198–207.
- [8] J.-P. Kreiß, E. Paparoditis, Autoregressive-aided periodogram bootstrap for time-series, *Ann. Statist.* 31 (2003) 1923–1955.
- [9] H.R. Künsch, The Jackknife and the bootstrap for general stationary observations, *Ann. Statist.* 17 (1989) 1217–1241.
- [10] E. Paparoditis, Frequency domain bootstrap for time series, in: H. Dehling, T. Mikosch (Eds.), *Empirical Process Techniques for Dependent Data*, Birkhäuser, Boston, 2002, pp. 365–381.
- [11] E. Paparoditis, D.N. Politis, The local bootstrap for the periodogram, *J. Time Ser. Anal.* 20 (1999) 193–222.
- [12] E. Paparoditis, D.N. Politis, Tapered block bootstrap, *Biometrika* 88 (2001) 1105–1119.
- [13] D. Politis, J. Romano, M. Wolf, *Subsampling*, Springer, Berlin, 1999.
- [14] D.N. Politis, J.P. Romano, T.-L. Lai, Bootstrap confidence bands for spectra and cross-spectra, *IEEE Transactions on Signal Processing* 40 (1992) 1206–1215.
- [15] M.B. Priestley, *Spectral Analysis and Time Series*, Academic Press, London, 1981.
- [16] P. Robinson, Automatic frequency domain inference on semiparametric and nonparametric models, *Econometrica* 59 (1991) 1329–1363.
- [17] J. Shao, D. Tu, *The Jackknife and the Bootstrap*, Springer, Berlin, 1995.
- [18] R. Shibata, An optimal autoregressive spectral estimate, *Ann. Statist.* 9 (1981) 300–306.
- [19] A.M. Zoubir, Bootstrapping spectral density estimates with kernel bandwidth estimation, in: Proceedings of the IEEE International Conference on Acoustics, Speech and Signal Processing, ICASSP-03, Hong Kong, 2003.
- [20] A.M. Zoubir, On confidence intervals for the coherence function, in: Proceedings of the IEEE International Conference on Acoustics, Speech and Signal Processing, ICASSP-05, Philadelphia, USA, 2005.
- [21] A.M. Zoubir, J.F. Böhme, Multiple bootstrap tests: an application to sensor location, *IEEE Transactions on Signal Processing* 43 (1995) 1386–1396.
- [22] A.M. Zoubir, D.R. Iskander, *Bootstrap Techniques for Signal Processing*, Cambridge University Press, Cambridge, 2004.